Surface & Coatings Technology 344 (2018) 111–120

Contents lists available at ScienceDirect

Surface & Coatings Technology

journal homepage: www.elsevier.com/locate/surfcoat

Thermal aging effects on mechanical and electrochemical properties of stainless steel weld overlay cladding

X.Y. Cao[a], P. Zhu[b], T.G. Liu[a], Y.H. Lu[a,*], T. Shoji[a,c]

[a] National Center for Materials Service Safety, University of Science and Technology Beijing, 30 Xueyuan Road, 100083 Beijing, China
[b] Suzhou Nuclear Power Research Institute Co. Ltd., 1788 Xihuan Road, 215004 Suzhou, China
[c] Fracture and Reliability Research Institute, Tohoku University, 6-6-01 Aoba AramakiAobaku, 980-8579 Sendai, Japan

ARTICLE INFO

Keywords:
Thermal aging
Stainless steel weld overlay cladding
Spinodal decomposition
Mechanical property
Intergranular corrosion

ABSTRACT

An investigation on mechanical property and electrochemical behavior of the cladding materials aged at 400 °C for different times was carried out by small punch test (SPT) and double loop electrochemical potentiokinetic reactivation (DL-EPR) test. The results showed that thermal aging contributed to spinodal decomposition and G-phase formation in the aged ferrite phase, as well as increase of nano-hardness of ferrite phase. The SP energy by the small punch tests decreased with increase of thermal aging time, which was related to the lattice distortions in G-phase and aged ferrite phase and their interactions with dislocations during deformation process. Thermal aging promoted corrosion and intergranular corrosion susceptibility of the cladding materials. Combined effects of G-phase and spinodal decomposition lowered intergranular corrosion resistance of the cladding material.

1. Introduction

Due to high mechanical property and corrosion resistance, Austenite stainless steel, including austenite and ferrite phases, were widely used as structural materials in many industries [1–3]. In addition, weld deposition of stainless steel on low alloy base metals, named as stainless steel weld overlay cladding, was widely selected to obtain the corrosion-resistant surface and avoid the premature failure of base metals. However, after a long term service at operated temperature (300 °C–500 °C),thermal aging embrittlement occurred in these stainless steels and cladding materials, leading to mechanical property degradation [4–6] and the reduction of corrosion resistance [7–11].

During thermal aging process, spinodal decomposition and G-phase formation were considered as the main microstructure change in the aged ferrite phase [12,13], wherein spinodal decomposition led to Fe-rich and Cr-rich domains formation, and the lattice parameters discrepancy among these domains were considered as the main factor for the hardening of ferrite phase [4–6] and properties degradation [8–11]. In addition, G-phase, the chemical composition is $Ni_{16}Mn_6Si_7$, was believed to promote the embrittlement of ferrite phase as reported by the previous work [12].

For mechanical property evaluation, small punch test (SPT) has received special attentions with its excellent sensitivity to various characteristics of materials [15,16], and the data obtained by SPT is in good agreement with the traditional impact and tensile tests [17,18]. Some researchers investigated the plasticity reduction of thermally aged materials by SPT and conventional tests, and confirmed the applicability of SPT for thermal aging embrittlement evaluation [18–20]. However, for the cladding material, few studies focused on the mechanical property change by SPT, in the meanwhile, the deformation behavior and mechanism of G-phase and spinodal decomposition were not clarified clearly during small punch tests, more investigation is needed.

Since spinodal decomposition induced Cr-depleted zone formation around Cr-rich phase and G-phase precipitates [7–11], electrochemical assessments especially intergranular corrosion tests were widely used to quantitative evaluation of the extent of degradation for thermally aged stainless steels [21,22]. Although many previous works have reported the pitting and intergranular corrosion behaviors of the aged stainless steels [23,24], the intergranular corrosion behavior of thermally aged weld overlay cladding draws less attention and its correlation with thermal aging embrittlement is not reported.

In our study, we investigated the mechanical property and electrochemical corrosion behavior of thermally aged stainless steel weld overlay cladding by SPT and DL-EPR test respectively. Scanning electron microscope (SEM) and back scattered electron microscope (BSE) were used to observe the microstructure of the cladding material after SPT and DL-EPR test, and the deformation behavior of the aged ferrite phase was observed by transmission electron microscopy (TEM) method. The degree of thermal aging embrittlement was evaluated by

* Corresponding author.
E-mail address: lu_yonghao@mater.ustb.edu.cn (Y.H. Lu).

https://doi.org/10.1016/j.surfcoat.2018.02.046
Received 11 December 2017; Received in revised form 6 February 2018; Accepted 14 February 2018
Available online 17 February 2018

Table 1
Welding parameters of SAW process.

Welding parameter	Voltage U/V	Current I/A	Heat input Q/(KJ/cm)	Welding speed V/(mm/min)
	25–27	700–800	68.8	170

using nano-hardness test and was correlated with the mechanical and electrochemical properties variations.

2. Materials and methods

2.1. Materials and welding

Three layers of E308L stainless steel weld strip were deposited on the A508 low alloy steel by submerged arc strip welding (SAW) to obtain the cladding metals. The corresponding welding parameters were listed in Table 1, wherein the equation for heat input calculation was $Q = {}^{UI}/_{V}$.

After welding, post-weld heat treatment (PWHT) was performed at 615 °C for 16 h to reduce the residual stress. Based on the previous works [1,2], the aging temperature in the range of 350 °C ~ 450 °C were widely selected and the corresponding aging time was up to 10,000 h. In our study, after PWHT, thermal aging treatment was carried out at 400 °C for 400, 1000, 5000 and 10,000 h, respectively, followed by furnace cooling. The chemical compositions of the weld and base metals are shown in Table 2.

2.2. Microstructure and nano-hardness

For microstructure observation, the 15 × 10 × 2 mm samples were cut from the top layer of the cladding plates. These samples were mechanically ground by silicon carbide papers to 5000 grit, and further polished using a 2.5 mm diamond paste, followed by etching with Kalling's reagent (10 g $CuCl_2$, 100 ml HCl and100 ml ethanol). Firstly, the distribution of δ-ferrite in the cladding material was observed by optical microscopy (OM), and secondly, the microstructural evolution resulting from thermal aging was observed by a FEI-F20 high resolution transmission electron microscopy (HRTEM) operated at 200 KV. TEM specimens were prepared with a twin-jet unit at 25V_{SCE} in a solution of 10% perchloric acid in 90% methyl alcohol. In addition, Digital Micrograph™ software was used to analyze HRTEM images and then, fast Fourier transformation (FFT) images and the corresponding crystal structure information were obtained.

In order to observe the effect of thermal aging on ferrite phase, nano-hardness test were carried out by a MTS Nano-Indenter DCM tester with 10 mN load, and the nano-hardness of the ferrite phases under the different aging conditions were the average value of at least three measured results.

2.3. Small punch tests

Before small punch tests, some 10 mm-diameter discs with a thickness of 500 μm ± 20 μm were cut, and subsequently ground up to 2000 grit and then, cleaned with distilled water. After samples preparation, an experimental device, consisting of a punch, a steel ball with a diameter of 2.5 mm and upper & lower dies used to hold the specimen, was used to test the mechanical property of the aged cladding material. The detailed schematic of the SPT device is shown in Fig. 1. During the process of SPT, the samples were deformed gradually until failure into the 4 mm-diameter lower die by the steel ball with a speed rate of 0.2 mm/min. At least three repeated tests for each aging condition were carried out at ambient temperature in air.

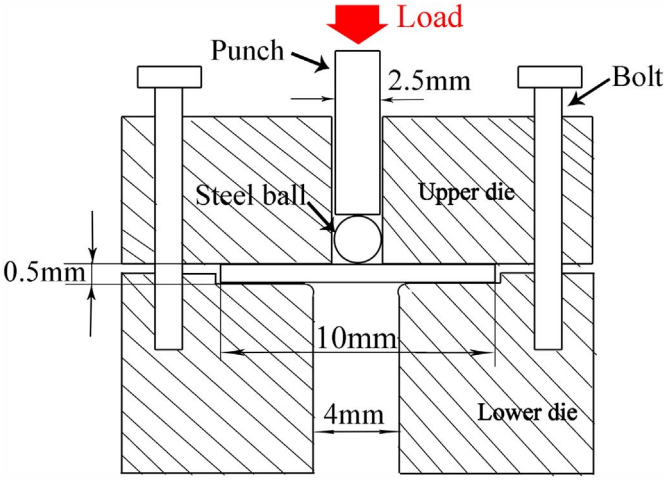

Fig. 1. Schematic of SPT (small punch test) device.

Since the final failure of the SP samples occurred after the load dropped to 80% of the maximum load according to the previous works [15–17], the tested samples in our study were deformed after the load dropped to 80% of the maximum load, and the corresponding the fracture surfaces and cross-section morphologies were obtained by SEM and BSE. In addition, TEM method was used to observe the deformation behavior of the aged cladding material after small punch test.

2.4. DL-EPR tests

Before DL-EPR test, The samples, with a size of 5 × 5 × 2 mm, were mechanically ground to 5000 grit gradually and then, embedded in epoxy resin to obtain a 0.25 cm^2 working electrode surface areas, and followed by polished using a 2.5 mm diamond paste. Potentiostat (CHI 6670) with a three-electrode system including a working electrode (sample), a saturated calomel reference electrode (SCE) and a Pt plate counter electrode was used during DL-EPR tests. All the DL-EPR tests were carried out at room temperature with the solution was 0.5 M H_2SO4 + 0.01 M KSCN. At the beginning of DL-EPR test, the test solution stabilized at open circuit potential (OCP) for 30 min and then, the potential was scanned from −0.5V_{SCE} to 0.3V_{SCE} in the positive direction, followed by reversing to −0.5 V_{SCE} in the negative direction with a scan rate of 1.67 mV·S^{-1}. Three repeated tests for each aging condition were carried out to confirm the reproducibility.

After DL-EPR tests, positive current peak value (Ia), and negative current peak value (Ir) were obtained and the Ir/Ia value was used to evaluated the Cr depletion degree of the cladding materials. In addition, the corresponding surface morphologies of the tested samples were observed by SEM equipped with energy dispersive spectrometer (EDS).

Table 2
Chemical compositions of weld and base metals (wt%).

Alloy	C	Cr	Ni	Si	Mn	S	P	Mo	N	Fe
E308L	0.024	20.34	10.52	0.86	1.42	0.007	0.014	< 0.005	0.095	Bal
A508	0.15	0.23	0.74	0.19	1.27	0.005	0.006	0.53	/	Bal